Reliability Analysis of Power Systems Integrated With High-Penetration of Power Converters

Bowen Zhang , *Student Member, IEEE*, Mengqi Wang , *Senior Member, IEEE*,
and Wencong Su , *Senior Member, IEEE*

Abstract—With the growing penetration of power electronic converters in power systems, the issue of reliability becomes more critical than ever before. This paper proposes a hierarchical reliability framework to evaluate the electric power system reliability from the power electronic converter level to the overall system level. On the converter level, the reliability model of a power electronic converter is developed based on the power electronic devices it is composed of, for which various hourly based input profiles and converter topologies are considered. On the system level, reliability metrics such as expected energy not served (EENS) and loss of load expectation (LOLE) are estimated through a non-sequential Monte Carlo simulation. Machine learning regression models, such as support vector regression (SVR), and random forests (RF) are implemented to bridge the nonlinear reliability relationship between two levels. The proposed framework is demonstrated through the modified IEEE Reliability Test System (RTS) 24-bus network. Numerical results show power converter reliability should be considered as an important factor when evaluating overall system reliability performance.

Index Terms—Power converters, power system reliability, machine learning, power electronics.

NOMENCLATURE

A. Parameters

P_r	Rated power of wind turbine generator (MW)
P_{pv}	Generated power of PV panels (MW)
P_{max}	Maximum power of PV panels (MW)
$P_{WT\_loss\_IGBT}$	IGBT power loss in WT system (MW)
$P_{WT\_loss\_diode}$	Diode power loss in WT system (MW)
$P_{WT\_loss\_conv}$	Converter power loss in WT system (MW)
$P_{pv\_boost\_IGBT}$	IGBT power loss in PV boost converter (MW)
$P_{pv\_boost\_diode}$	Diode power loss in PV boost converter (MW)
$P_{pv\_boost\_inductor}$	Inductor power loss in PV boost converter (MW)

V_P	Primary side voltage of wind turbine (V)
V_{DC}	DC link voltage in wind turbine (V)
V_{CEO}	Threshold voltage drop on the IGBT (V)
V_{FO}	Threshold voltage drop on the diode (V)
f	Grid frequency (Hz)
f_{sw}	Switching frequency (Hz)
r_{CE}	IGBT equivalent resistance (Ω)
r_F	Diode equivalent resistance (Ω)
r_{es}	Main inductor equivalent resistance (Ω)
M	Modulation ratio
S_0	Maximum radiation of PV panels (W/m^2)
φ	Angle between voltage and current
E_{on}	IGBT on-state energy losses (mJ)
E_{off}	IGBT off-state energy losses (mJ)
E_{rec}	Diode rated switching energy loss (mJ)
T_j	Component junction temperature (***)
R_{sa}	Thermal resistance from heat sink to ambient (K/kW)
R_{jh}	Thermal resistance from junction to heat sink (K/kW)
π_T	Thermal stress factor
λ	Component failure rate (FIT)
γ_0	Temperature coefficient
T_0	Time span $T_0 = 8760$ hours

B. Variables

v_t	Actual wind speed at time t (m/s)
T_t	Ambient temperature at time t (F)
S_t	Solar radiance at time t (W/m^2)

C. Acronyms

RES	Renewable energy source
PV	Photovoltaic
WT	Wind turbine
CHP	Combined heat and power units
FTA	Fault tree analysis
MCM	Markov chain modeling
PMSG	Permanent magnet synchronous generator

I. INTRODUCTION

IN RECENT years, modern power system structures deployed with local available renewable energy resources (RESs), including solar photovoltaic (PV) generators, wind turbines (WTs), and combined heat and power units (CHPs), have been more favorable, compared to traditional centralized controlled

Fig. 1. A prediction of the future power system structure.

power systems. Utilizing the power generated from RESs can reduce the carbon emissions in the environment and significantly increase system operation flexibility [1]. As illustrated in Fig. 1, it is foreseeable that conventional generators will be replaced by different RESs in the future and RESs with smaller capacity, such as rooftop PVs will be widely implemented. As a result, however, the entire system reliability will become more complicated. Specifically, more power conversions will be inevitably required between different energy levels. Whether the generated power from RESs can be efficiently, desirably and reliably converted to the load side is greatly dependent on the performance of the connected power electronic interfaces. The penetration of power electronic converters has brought a huge challenge to the existing power system structure from a reliability point of view.

The main purpose of conducting reliability evaluation in power systems is to provide quantitative analysis with various indices for improving system operation and future planning [2]. Different methods have been applied for power system reliability evaluation. Analytical methods, such as fault tree analysis (FTA) [3] have been utilized for optimal transmission system planning. The authors in [4] proposed a system evaluation method based on the minimum path and calculated the reliability indicator on various load points. Simulation methods, such as the Monte Carlo method, have been used [5] to sample the component states in a power system. In [6], an artificial neural network (ANN) was implemented to predict the future reliability of a distribution system through historical data.

Many of the aforementioned methods have been refined to accommodate the RES contingencies and diverse load demands in power systems. However, failures caused by power converters connected to RESs have been mostly considered as constant or even ignored in most published research works. Authors in [7] investigated the age-related failure of power transformers and assumed 100% reliable for other units. In [8], the authors proposed time-varying reliability models for generating units under high penetration of wind power but didn't consider the potential failure of those connected converters. A reliability assessment was conducted in [9] for components in large scale PV systems, and the inverter failure rate was a constant throughout

a year. In addition, the reliability evaluation of power systems is also dependent on various defined indicators. In addition, the reliability evaluation of power systems is also dependent on various defined indicators. Classic system reliability indices, such as expected energy not supplied (EENS) and loss of load expectation (LOLE), have been widely used for system reliability evaluation [10]. In [11], a series of novel metrics is proposed to understand system reliability performance from various perspectives, including resiliency and power planning. Meanwhile, reliability metrics related to power electronic interfaces, such as semiconductor failure rates and converters' overall power availability have not generated much attention.

That said, researchers in the power electronics field, have concentrated on evaluating the reliability model from both the semiconductor device level and the overall converter level for years. The paper [12] provided a comprehensive review on the reliability issues of semiconductor devices in power converters. Authors in [13], [14] investigated the reliability of a DC-DC converter where time-to-failure models of semiconductors such as MOSFET and IGBT are included. In [15], the authors presented a reliability comparison among three types of converters used in the grid-connected wind turbines. Meanwhile, many papers have investigated power converter reliability performance when a system is connected to uncertain RES supplies [16]–[20]. In [16], [17], reliability and cost analyses of a DC-DC boost converter connected to PV panels were conducted. Authors in [18] proposed a back-to-back power converter for wind turbines to improve the system reliability. Considering the thermal loading and lifetime estimation, a reliability evaluation for critical devices under a typical WT converter topology was performed in [19]. In [20], converters connected to a hybrid PV-wind system were evaluated from efficiency and reliability perspectives. To mathematically estimate power converter reliability, several quantitative methodologies were presented in [21], [22]. In [22], novel or optimized converter designs were proposed to enhance not only the device but also the RES reliability performance. In summary, many papers mainly focus on whether the power converter can reliably convert the input power to the grid when faced with the fluctuation on the generation side; however, efficient power conversion from RESs can only guarantee that all the available energy from the environment is injected into the power system. Whether the generated power can be successfully delivered, and is sufficient enough to satisfy the load demand, are still questionable.

Based on the above-mentioned surveys, it can be concluded that many research works have investigated reliability from a specific aspect either the power system or the power electronics field. In terms of reliability assessment, power electronic interfaces, namely power converters, play an increasingly important role in recent years with their foreseeable penetration in modern power systems. Thus, the reliability modeling of power converters is essential when evaluating the system reliability. Meanwhile, the failure-related reliability of power converters is greatly dependent on the semiconductor devices. The proposed framework, therefore, builds a library of failure rates for different semiconductor devices, and calculates all converters' reliability considering different converter topologies.
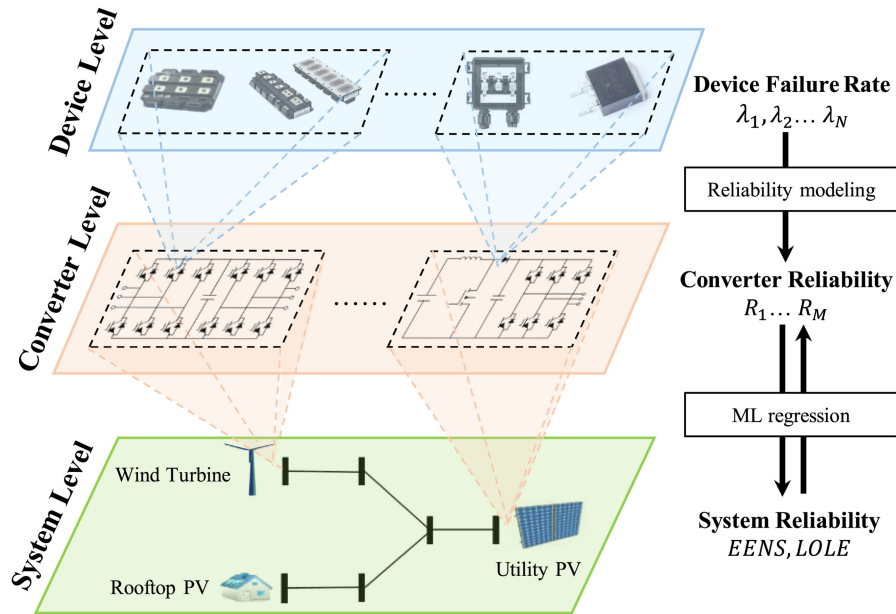
Fig. 2.   The proposed hierarchical power system reliability assessment framework.

The overall system reliability is greatly dependent on all converters' performance. However, there is a lack of research regarding how the converter level reliability will affect the system reliability, i.e., the reliability relationship between converter and system level. Further, due to the increasing complexity of modern power systems, this reliability impact from converter to system level remains unknown and cannot be analytically solved.

Thus, another purpose of this paper is to bridge this gap between two levels by implementing machine learning (ML) regression analysis. It is well known that regression analysis can establish a relationship among input features and output labels [23], so we consider applying this methodology for two reasons. First, the reliability indicators of the device and system level are all continuous instead of categorized variables. Second, it is certain that the relationship between two levels is nonlinear. Regression modeling has much better capability to build a nonlinear relationship among input/output data compared with using a look-up table [24]. Besides, the complexity of input features increases when more power converters are considered in a power system. The regression method can handle adding any parameter as an input feature of the model, such that the modeling scalability and flexibility are greatly improved.

In this paper, we propose a machine learning-based model for the system reliability assessment. As shown in Fig. 2, in the device level, the failure rate model of component is employed under given climate conditions. Several semiconductor devices such as IGBT and diode are included. Then, in the converter level, based on those components' failure rates and converter topologies, we consider modeling the reliability of different power electronic converters connected to all RESs. After modeling all converters reliability, the system reliability is generated and evaluated by applying system reliability indicators. ML regression techniques are integrated to explore the reliability relationship between

converter and system level. This comprehensive procedure is explained in the following sections. The main contributions of this paper can be summarized as follows.

1) The proposed hierarchical reliability framework consists of three levels. We build a comprehensive library of failure models of a wide range of semiconductor devices, considering their thermal/physical dynamics and environmental conditions. Based on the power converter topology, we apply a combination of device failure rates to build a composite reliability model of each power converter.

2) Due to the proliferation of power converters in a modern power system, their individual reliability indices greatly affect the overall power system performance. Therefore, the ability to generalize the reliability evaluation of converter-dominated power systems is highly valuable and could accelerate the deployment of new power electronics technologies. This paper presents for the first time an integrated three-layer framework to obtain a fundamental understanding of the inter-relationships among device failure rates, power converter reliability, and power system reliability.

3) A modern power system usually involves a large number of components and sub-systems. A fundamental understanding of the reliability impacts from converter failure to the overall system performance is still an unsolved puzzle. Conventional approaches are reliant on human-expert prior knowledge that may not be quantitative. To collectively solve these challenges, this paper leverages modern machine learning (ML) techniques to provide a baseline tool that can capture the dependence structure for a large group of components and evaluate the reliability indices of converter-dominated power system at scale. The knowledge obtained from ML can provide theoretically sound yet easy-to-implement guidelines for power system

operators to mitigate eventual failures. It is worth noting that it is not our focus to deliver a commercial-grade ML tool. The goal is, rather, to provide a baseline platform to the research society so that interested users can further study the reliability performance of converter-dominated power systems by incorporating more advanced ML algorithms.

The rest of the paper is organized as follows. First the basic reliability concepts in power systems and power electronics are presented in Section II. Section III presents the formulation of power converter reliability. The Monte Carlo simulation and a system overview are provided in Section IV. Information about ML and multiple regression models is presented in Section V. Reliability performance of the system under the modified IEEE-RTS 24 bus network is analyzed in Section VI. Finally, Section VII summarizes the conclusions and future works.

II. RELIABILITY CONCEPTS

Reliability is a specific measurement and an inherent characteristic of a device or system which describes its ability to perform its intended function within a period of time [1]. According to this definition, a device/system is considered reliable if its regular performance can be retained during a specified time interval. On the contrary, if failures happen during the interval and the performance cannot meet the pre-defined requirement, the device/system is considered unreliable, and maintenance is required to improve its reliability. To quantitatively measure the reliability of a device or system, different reliability indicators have been developed. Furthermore, if a system is composed of several sub-systems, its reliability evaluation becomes complicated because each sub-system should be evaluated first with corresponding reliability indicators.

An electric power system is a typical complex system that consists of various components and sub-systems. The system function that is, meeting the power demand on all load points should be guaranteed at all times. As a result, classic indices such as EENS and LOLE were developed to evaluate system reliability from energy and load loss perspectives. A system with a high value of EENS/LOLE is considered an unreliable system. For an ideal power system, the power generation is sufficient and the load demand is satisfied all the time, such that both EENS and LOLE can reach zero; however, contingencies and failures can happen at any component during any time under a modern power system, resulting in an increase on those indices. Components, including generators, transmission lines, and load points, can fail due to random outages or aging issues. Moreover, with the development of renewable energy technology, RESs such as WTs and PV systems are replacing traditional diesel generators in today's power systems. Their power generations are largely dependent on time-variant ambient conditions, though, which introduces more uncertainty into power systems and may ultimately affect system reliability. Thus, evaluating the components reliability is essential when assessing the reliability performance of a power system.

As one of components in a power system, the power electronic converter has not garnered much attention when evaluating system reliability performance. However, accompanied by increasing RES implementation in modern power systems, the power electronic converter is necessarily equipped as an interface to deal with power conversion. The generated power from a WT or PV source can be successfully injected into the grid only if the power converter operates correctly at all times. Thus, the reliability of power converters is of great importance as it may affect the entire system's reliability. In addition, a power converter is composed of various semi-conductor devices. For each of these devices, the device failure rate is usually used as one of the reliability indices to evaluate its reliability. Furthermore, the time-varying operating condition and thermal stress on a device will greatly affect its failure rate. In conclusion, the reliability of a power converter should be modeled based on its critical devices and should be taken into consideration when evaluating power system reliability.

Therefore, with the increased penetration of RESs and power converters in modern power systems, reliability can be modeled hierarchically with two levels. First, the WT/PV converter reliability modeling is built based on various devices considering thermal effects and operating conditions. The converter topologies are also considered to determine the total number of devices. Then, together with other components' reliability, the converter reliability is incorporated into the system level analysis and the system reliability indices, including EENS and LOLE are estimated. The detailed reliability modeling for the converter level is described in the next section.

III. CONVERTER RELIABILITY FORMULATION

First, the reliability of each power converter connected to a RES (WT or PV system) should be practically quantified. As in equation (1), the reliability value $R(t)$ is traditionally calculated from the failure rate λ, where λ is independent of time and treated as a constant value [10].

$$R(t) = e^{-\lambda t} \tag{1}$$

However, surveys show that the values of failure rates are greatly affected by various factors, including ambient variations and device thermal loading [11]. To consider those factors which have potential reliability impact on a power converter, the general FIDES model is used in this paper, and expressed in the following equation (2) [25], where Π_{PM} is the contribution from quality and technical control over manufacturing of the component. $\Pi_{Process}$ consists of all processes, from specification to field operation and maintenance. These two parameters are assumed to be one in the proposed modeling process.

$$\lambda = \Pi_{PM} \Pi_{Process} \lambda_{Phy} \tag{2}$$

λ_{Phy} is of paramount importance in this equation which takes all component states into account, and is calculated by:

$$\lambda_{Phy} = \sum_i^{States} \left[\frac{t_{annual}}{T} \right]_i \Pi_i \lambda_i \tag{3}$$

where t_{annual} is the duration of the ith state throughout the time span T. Π_i is the induced overstress electrical factor which is defined by the user and are specific to each component [22]. λ_i
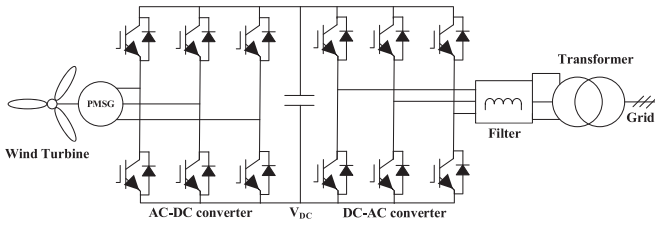
Fig. 3.   Typical wind power system.
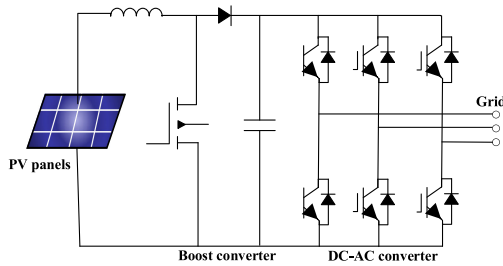
Fig. 4.   PV system with dc-dc boost converter and dc-ac inverter.

is calculated depended on the specific component and is used to estimate its final component failure rate. The detailed process is presented below.

A. Reliability Model of WT Converters

A typical wind power system is considered, consisting of a permanent magnet synchronous generator (PMSG), a generator-side inverter, a dc link, and a grid-side inverter, as shown in Fig. 3. The WT output power varies with the wind speed and angle. This results in the variation of device power losses, and ultimately affects the device failure rate. Thus, hourly based wind speed data is collected to determine the output power $P_{wt,t}$ at hour t which is estimated in equation (4), where v_t is the wind speed, P_{rated} represents the rated capacity, v_{ci}, v_r, and v_{co} are the cut-in, rated, and cut-out wind speeds of the WT system, respectively. Thus, hourly based wind speed data is collected to determine the output power $P_{wt,t}$ at hour t [26].

$$P_{wt,t} = \begin{cases} 0, & 0 \le v_t \le v_{ci} \\ (A + Bv_t + Cv_t^2)\, P_{rated}, & v_{ci} \le v_t \le v_r \\ P_{rated}, & v_r \le v_t \le v_{co} \\ 0, & v_t \ge v_{co} \end{cases} \quad (4)$$

As shown in equation (4), a second-order function is applied to estimate this non-linear function where v_t is the wind speed, P_{rated} represents the rated capacity, v_{ci}, v_r, and v_{co} are the cut-in, rated, and cut-out wind speeds of the WT system, respectively [27].

Then, the power losses of power electronic devices in the WT can be estimated. Critical semiconductors considered here are diodes and IGBTs. The total device power losses consist of conduction loss and switching loss. Both losses are determined by various parameters. For example, the diode/IGBT conduction loss is related to its resistance and voltage drop, while switching

loss is related to the switching frequency [19].

$$P_{WT_{IGBT_{con}}} = I_{wt}\, V_{CEO} \left(\frac{1}{2\pi} + \frac{M\cos\varphi}{8} \right)$$
$$+ I_{wt}^2 r_{CE} \left(\frac{1}{8} + \frac{M}{3\pi}\cos\varphi \right) \quad (5)$$

$$P_{WT_{diode_{con}}} = I_{wt}\, V_{F0} \left(\frac{1}{2\pi} - \frac{M\cos\varphi}{8} \right)$$
$$+ I_{wt}^2 r_F \left(\frac{1}{8} - \frac{M}{3\pi}\cos\varphi \right) \quad (6)$$

Equations (5) and (6) express the calculation of the conduction loss of a diode and an IGBT, respectively, where I_{wt} represents the peak phase current and can be calculated from P_{wt}; V_{CEO}, V_{F0} are the threshold voltage drops on the IGBT and diode respectively; r_{CE}, r_F denotes the resistances of the IGBT and diode; M represents the modulation ratio; and φ is the angle between the voltage and current.

$$P_{WT\_IGBT\_sw} = \frac{1}{\pi}\, f_{sw}\, (E_{on} + E_{off}) \frac{I_{wt} V_{DC}}{V_{ref\_IGBT} I_{ref\_IGBT}} \quad (7)$$

$$P_{WT\_diode\_sw} = \frac{1}{\pi}\, f_{sw} E_{rec} \frac{I_{wt} V_{DC}}{V_{ref\_diode} I_{ref\_diode}} \quad (8)$$

The switching loss can be calculated as in (7) and (8), where E_{on} and E_{off} are the IGBT energy losses of the ON and OFF state; V_{ref_IGBT} and I_{ref_IGBT} are the reference commutation voltage and current of the IGBT; V_{ref_diode} and I_{ref_diode} are the reference commutation voltage and current of the diode; and E_{rec} is the rated switching energy loss of the diode.

The total power loss of a diode/IGBT can be derived by adding its conduction loss and switching loss, shown in (9) and (10), where the subscript *cd* stands for the conduction loss, and *sw* indicates the switching loss. The detailed equations for calculating P_{IGBT_cd}, P_{IGBT_sw}, P_{diode_cd} and P_{diode_sw} are provided below.

$$P_{loss\_IGBT} = P_{IGBT\_cd} + P_{IGBT\_sw} \quad (9)$$

$$P_{loss\_diode} = P_{diode\_cd} + P_{diode\_sw} \quad (10)$$

There are two converters in this WT system, namely the generator-side inverter and the grid-side inverter. Based on the converter topology shown in Fig. 3, the number of diode/IGBT can be determined. All components are connected in series from a reliability point of view. Thus, the total power loss on these two converters $P_{WT\_conv\_loss}$ can be estimated by the power loss of all diodes and IGBTs:

$$P_{WT\_conv\_loss} = \sum_{n=1}^{n_D} P_{loss\_IGBT} + \sum_{n=1}^{n_G} P_{loss\_diode} \quad (11)$$

where n_D and n_G represent the total number of diode and IGBT, respectively.

Since the thermal behavior is one of the important factors that has an influence on the device failure rate, the calculated $P_{WT\_conv\_loss}$ and hourly based ambient temperature data are applied to estimate the junction temperature and the thermal

stress factor of a diode and of an IGBT. The thermal resistance and the temperature cycling factor for each diode and IGBT are also considered.

$$T_{j_{IGBT}} = T_C + R_{sa_{IGBT}} P_{WT_{loss_{conv}}}$$
$$+ R_{jh\_IGBT} P_{WT\_loss\_IGBT} \quad (12)$$

$$T_{j_{diode}} = T_C + R_{sa_{diode}} P_{WT_{loss_{conv}}}$$
$$+ R_{jh\_diode} P_{WT\_loss\_diode} \quad (13)$$

Equation (12) and (13) calculate the junction temperature of a diode and an IGBT, where T_C is the ambient temperature, and R_{sa} and R_{jh} are the thermal resistances from heat sink to ambient/from junction to heat sink, respectively.

The thermal stress factor π_T for a diode or an IGBT can be derived in (14) and (15).

$$\pi_{T\_IGBT} = \exp\left[1925\left(\frac{1}{298} - \frac{1}{T_{j\_IGBT} + 273}\right)\right] \quad (14)$$

$$\pi_{T\_diode} = \exp\left[3091\left(\frac{1}{298} - \frac{1}{T_{j\_diode} + 273}\right)\right] \quad (15)$$

The temperature cycling factor π_{TC} for a diode or an IGBT can be expressed by (16).

$$\pi_{TCi} = \gamma \left(\frac{12N_s}{t(i)}\right) f(\Delta T_b)$$
$$\times \exp\left[1414\left(\frac{1}{313} - \frac{1}{T_{b\_max} + 273}\right)\right] \quad (16)$$

where γ and $f(\Delta T_b)$ have a specific value/expression for a diode or an IGBT, and their values can be found in [22].

Then, the failure rate model for a semiconductor can be derived, by utilizing all the calculated results from above and the method in [22], where the above-mentioned factors that potentially affect the reliability performance for the component failure rate estimation are considered. Other factors such as radiation, heat and electrical stresses, wear-out effect, and production quality are also included. The failure rate models of a diode or an IGBT are expressed in (17):

$$\lambda_{j,t} = \sum_{i}^{N_s} \left(\lambda_{0Th}\pi_{Tj,t} + \lambda_{0TC}\pi_{TCj,t}\right) \pi_{In}\pi_{Pm}\pi_{Pr} \quad (17)$$

where $\lambda_{j,t}$ represents the failure rate of component j at time t, N_s is the number of component states; λ_{0Th} and λ_{0TC} are two base failure rate elements of a component, respectively; $\pi_{Tj,t}$ and $\pi_{TCj,t}$ are the thermal stress factor and the temperature cycling factor of component j at time t, respectively; π_{ln} is the overstress factor used to represent the overstress contribution, determined by the coefficient sensitivity to overstress and the component application field; π_{Pm} represents the factor of component quality; and π_{Pr} is the factor of reliability control reflecting the aging status in the component's life cycle.

$$R_{WT_{conv}}(t) = e^{-\left(\sum_{j=1}^{N_j} \lambda_{j,t}\right)t} \quad (18)$$

Finally, the failure rate of the WT converter can be derived and the converter reliability can be expressed as in (18), where N_j represents the total number of devices.

B. Reliability Model of PV Converters

As shown in Fig. 4, a typical PV system, as considered in this paper consists of a PV array, a dc-dc boost converter, and a dc-ac inverter.

Similar to a WT system, the output power of the PV system has a close relationship with the device failure rate. Thus, hourly based input data, such as solar radiance and ambient temperature are collected. Assuming a maximum power point tracking (MPPT) mechanism, the power produced by PV panels is calculated in equation (19), where $P_{pv,t}$ is the power generated by the PV panels at time t; S_t is the input solar radiation intensity; S_0 represents the maximum radiation; P_{max} is the maximum power under standard test conditions; γ is the temperature coefficient; T_t is the input ambient temperature, and T_0 represents the standard temperature.

$$P_{pv,t} = \frac{S_t}{S_0} P_{max} [1 + \gamma_0(T_t - T_0)] \quad (19)$$

Converters considered in this PV system include a boost, and a dc-ac inverter. Three components, namely a diode, an IGBT and an inductor, are considered in the PV boost converter. The components power losses in the dc-dc boost converter, including conduction loss and switching loss, are calculated similarly compared to WT converter modeling and are presented in (20)-(22), where $R_{DS(on)}$ is the resistance between the drain and source when the switch is on; f_s is the switching frequency; r_F is the equivalent resistance of the diode; V_F is the forward voltage drop; and r_{es} is the equivalent resistance for the main inductor.

$$P_{pv_{boost_{IGBT}}} = R_{DS(on)} I_{in}^2 + \frac{1}{2}V_{out}I_{in}(E_{on} + E_{off})f_s \quad (20)$$

$$P_{pv\_boost\_diode} = I_{out}^2 r_F + I_{pv}V_{F0} \quad (21)$$

$$P_{pv\_boost\_inductor} = I_{in}^2 r_{es} \quad (22)$$

The operating temperature of the main inductor is determined by equations (23)–(24), where T_{HS} is the hot spot temperature of the inductor, which is a function of its power dissipation and radiating surface area A. T_C represents the case temperature.

$$T_{HS} = T_C + 1.1\Delta T \quad (23)$$

$$\Delta T = 125 P_{pv\_boost\_inductor}/A \quad (24)$$

The reliability of PV converter is then presented in (25), where N_m represents the total number of devices used in the PV converter, and $\lambda_{m,t}$ is the failure rate of component m at time t.

$$R_{PV_{conv}}(t) = e^{-\left(\sum_{j=1}^{N_m} \lambda_{m,t}\right)t} \quad (25)$$

IV. SYSTEM LEVEL NON-SEQUENTIAL SAMPLING AND OVERVIEW

In the proposed power system network, the system-level reliability modeling is realized through a non-sequential Monte Carlo sampling method, which requires less computational time and memory compared with a sequential sampling method [28],
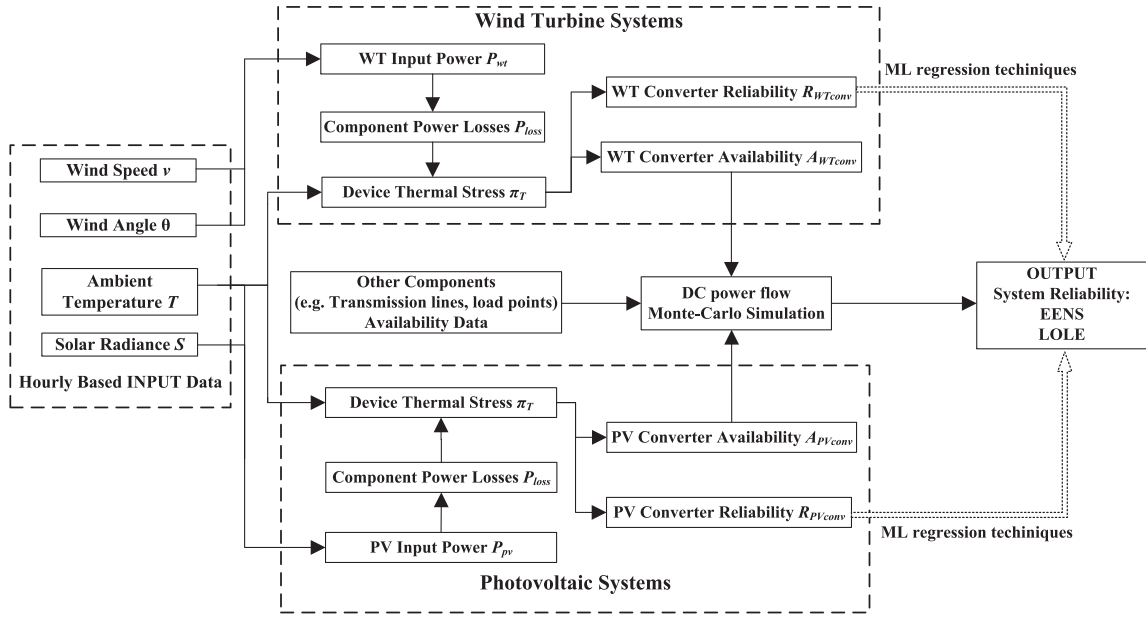
Fig. 5. The flowchart of the proposed power system reliability assessment.

[29]. For each hour, the entire system state is determined through sampling the probability of all components' states. It is assumed that the WT/PV generators have multi states depending on their power output level, and other component has two states: up and down, and that the components are independent from each other. It is worth noting that the components are assumed to be independent because our main focus is to investigate the reliability effect from a power converter perspective. Partially dependent scenarios, such as a cascading failure, are not considered in this paper.

Since the failure rate is calculated through hourly based data, each component i has a failure rate $\lambda_{i,t}$ at hour t. The repair rate μ_i is relatively stable and considered as a constant. Each component's up and down state probability can be calculated using (26) and (27).

$$P_U\ (i,t) = \frac{\mu_i}{\lambda_{i,t} + \mu_i} \tag{26}$$

$$P_D\ (i,t) = \frac{\lambda_{i,t}}{\lambda_{i,t} + \mu_i} \tag{27}$$

Thus, when conducting a non-sequential sampling each hour, each component state can be sampled independently, and the entire system state is determined by the combination of all components' states. Then, DC load flow based linear programming is adopted each hour to calculate the power flows, with the advantages of easy implementation and relatively low computational cost. Repeat the sampling procedure for a number of simulations until the stopping rule is satisfied. Finally, the estimated system reliability indicators, such as EENS and LOLE are calculated for system analysis.

In Fig. 5, an overview of the proposed framework is presented. First, we collect the hourly-based input data including wind speed, wind angle, solar radiance, and ambient temperature, to

estimate the generation power of the WT/PV system throughout one year. Since the power converter consists of various devices, each component's power loss and thermal stress are calculated to derive the time-variant failure rate for each component. Afterwards, the number of each component used in a WT/PV converter is determined based on the converter topology such that all components failure rates are accumulated and the converter reliability can be predicted. Then, we also consider other reliability data to estimate all component states in the power system. As shown in Fig. 5, other system components include, but are not limited to, diesel generators, transformers, transmission lines, and load demand. The failure rates of other system components are assumed to be constant. Thus, after estimating the hourly failure rates of all power converters, all components availability/unavailability can be calculated through the equation (26) and (27). After determining all component states, we conduct the DC power flow to check the balance of power supply and demand. DC power flow method is a widely used tool for power system analysis which substantially save the computational cost. If part of the load demand is not satisfied, the energy loss will be converted and added onto the system reliability indicators (EENS, LOLE). The reliability mapping between the device and system level is realized through ML regression techniques, which are introduced in the next section.

V. RELIABILITY MAPPING THROUGH REGRESSION TECHNIQUES

The development of data science has introduced more applications of artificial intelligence (AI), and ML techniques in diverse fields in recent years [30]. In this paper, ML regression techniques are implemented for converter level and system level reliability due to the following reasons. First, to examine the potential effect on system reliability from a power converter

perspective, the relationship between power converters and the overall system reliability data are worth investigating; however, due to the high system complexity, this kind of relationship is usually nonlinear such that it is difficult to derive an analytical expression. The ML method is capable of dealing with the non-linear data relationship, though, because one of the impressive ML capabilities is to approximate the input/output data relationship with arbitrary precision [31]. Second, the relationship may vary as more converters are considered in the power system reliability analysis. ML provides the flexibility for additional parameters to be embedded as another input feature such that the nonlinear relationship can be generalized [32]. Third, system reliability indicators such as EENS and LOLE are considered as the system output labels and they are all continuous. In this work, regression models are preferable compared to classification techniques where the output variable is usually discrete. In this section, basic fundamentals of ML regression and the proposed reliability mapping model are presented.

A. Theory

From a statistic perspective, the relationship mapping between device and system level reliability data can be modeled as a regression problem. The system reliability indicators are usually treated as system outputs and the reliability of each power converter is considered as one of the input features. The regression logic is described as follows.

Assume that there are n pairs of training data in a set $\{(x_k, y_k), k = 1, 2, \ldots, n\}$, where x_k is the input feature vector. x_k usually contains an array of data where all data are surrounding a target sample point [28]. The value of this target sample point is calculated from x_k during the testing procedure, and is compared with y_k (y_k is continuous), the true value of this sample point. Thus, accuracy is achieved through this comparison. The mapping between input features and output labels is used to investigate an appropriate function from x to y such that when x_k is known, the value of y_k can be predicted. In the proposed RTS network, all converters reliability data are considered as the input features which are injected into a regression model, and the system reliability indicators are the output labels. The selected ML regression methods are support vector regression (SVR) and random forests (RF). It is worth noting that there are other ML algorithms and they may have comparative performance. The purpose of this paper is not to find the optimal regression model, but to provide a potential reliability mapping from the device level to the system level through ML techniques.

B. Support Vector Regression

SVR has mainly been developed for handling nonlinear regression problems. This algorithm is adapted from the ML classification paradigm, namely the support vector machine (SVM) which is operated by maximizing the margin of the decision boundary [33]. In SVR, the first step is to map the input features $x = \{x_1, x_2, \ldots, x_n\}$ (with n power converters considered, for example) into an n-dimensional kernel-induced feature space

---

Algorithm 1: Reliability Mapping Through ML Regression Techniques.

Input: Calculated power converter reliability data x, system reliability indices y.
Output: Predicted system reliability indices
Training:
1 A data set is created where vector x denotes all power converter reliability at hour t and y stands for the system reliability index (i.e., EENS, LOLE).
2 Create two ML regression models:
3 $\hat{f}_{SVR} = SVR\,()$
4 $\hat{f}_{RF} = RandomForestRegression\,()$
5 Input all the x and y pairs to each model for training The ratio of training to testing data is 8:2.
Testing:
6 The trained models are applied to the remaining x data and derive the prediction of $\hat{y}$.
7 Use typical indices, such as RMSE and R-squared, to evaluate the mapping models

---

through a fixed mapping method where they are linearly correlated with the output labels. Thus, the SVR model can be described by the following notation:

$$f\,(x) = \sum_{k=1}^{n} \hat{y}_k g_k\,(x) + b \qquad (28)$$

where $\hat{y}_k$ is the predicted system reliability value, $g_k(x)$ denotes the nonlinear transformation, and b stands for the predicted bias value. A cost function is required for the SVR formulation. A robust ε-insensitive loss function is adopted. Detailed mathematical information can be found in [33].

C. Random Forests

RF is an ensemble learning method developed for improving classification and regression trees through combining a large set of decision trees [34]. Each individual tree is built based on a random subset of the input variables and the predicted output value depends on the average prediction of all aggregated trees. Specifically, an input vector $x = \{x_1, x_2, \ldots, x_n\}$ is given to build the forest. A set of m trees $\{T_1(x), T_2(x), \ldots, T_m(x)\}$ is created and all trees predict the output $\{\hat{y}_1 = T_1\,(x), \ldots, \hat{y}_m = T_m\,(x)\}$. To derive the final result, all trees' predictions are aggregated, and the average value is calculated as in (29). The growing procedure of each tree can be found in [35].

$$\hat{f}\,(x) = \frac{1}{m} \sum_{k=1}^{m} \hat{y}_k\,(x) \qquad (29)$$

The main steps of the proposed regression mapping are provided in Algorithm 1. The root-mean-square error (RMSE) and R-squared are used to evaluate the performance of both regression models. RMSE is a standard measure of error when a model predicts quantitative data [32]. The lower RMSE value is, the better prediction is indicated in this regression model. On
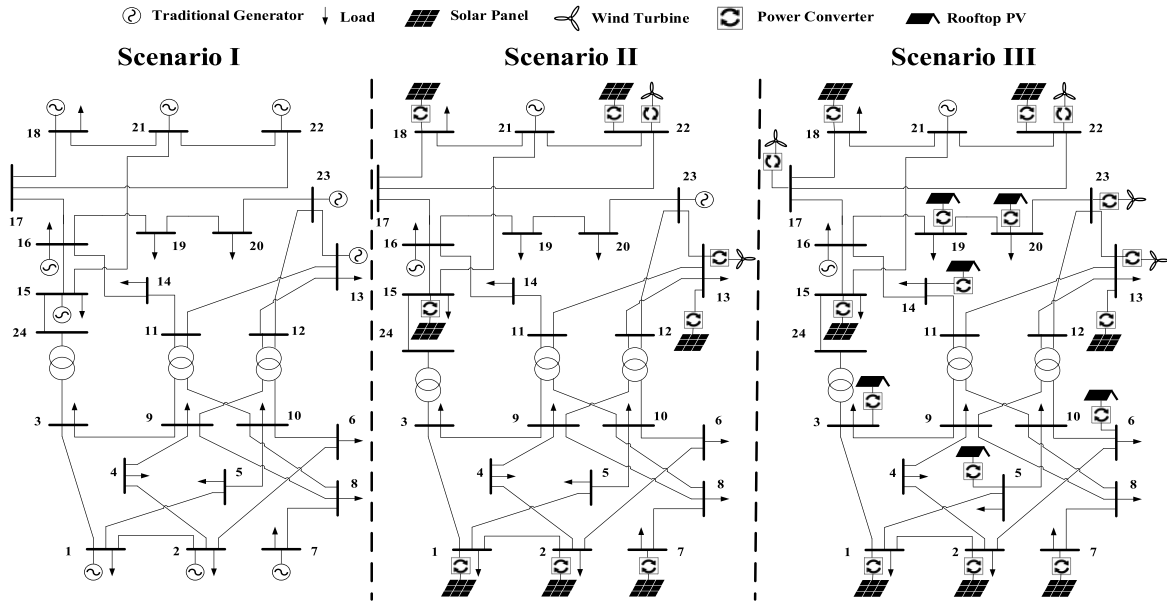
Fig. 6.   The illustration of RES/power converter penetration in the RTS network. Generators are all conventional in scenario I. Several RESs and connected power converters are implemented in scenario II. More RESs, including rooftop PVs, and power converters are considered in scenario III.

the other hand, R-squared is a statistical measure that indicates how much a variation of a dependent variable is explained and it ranges from 0 to 1. In general, if the R-squared value reaches 1, it represents that the implemented regression model is well fitted to the input/output data set. On the contrary, when the R-squared reaches 0, it indicates that the regression model does not fit the data at all.

VI. NUMERICAL ANALYSIS

The proposed framework was validated on a system with the following configuration: Intel(R) Core(TM) 16 GB 2.30 GHz. The non-sequential MC simulation was performed in Matlab 2019b, and ML regression models were implemented through Python scikit-learn. The collected hourly based data, such as wind speed, solar radiance, and ambient temperature, are provided in [36].

A. System Description

In this paper, a modified IEEE RTS-24 bus network as shown in Fig. 6, is used as the test system. To investigate the penetration of RESs and power electronic converters, three scenarios are considered to reflect converter penetration in a power system:

1) Scenario I: In this scenario, the original RTS is applied as shown on the left side of Fig. 6, where all generators are conventional (e.g., diesel, thermal). Thus, traditional generators dominate the power system generation in this case, and the system reliability is evaluated without considering the RESs and power converters. Other components such as transmission lines and load points are equipped with constant failure rates. The detailed reliability data and load model are provided in [36].

2) Scenario II: This scenario mimics the proliferation of RESs in an RTS network that renewable technology has been developing rapidly in recent years. Specifically, two WT and seven PV systems are implemented to replace conventional generators on different buses, as shown in the middle of Fig. 6. The WT and PV converter reliability models were presented in Section III with a small rated capacity, such as 2 MW and 0.5 MW, respectively. Thus, the reliability model of each power converter implemented in this scenario can be obtained by combining the reliability of each individual WT/PV converter. For instance, the reliability of a 25.9 MW PV on bus 1 can be obtained by combining 52 small converter reliability models where each has a capacity of 0.5 MW.

3) Scenario III: This scenario assumes that renewable technologies are sufficiently developed for industrial/residential use in the future, as presented on the right side of Fig. 6. Two more WT systems are considered on buses 17 and 23, respectively. Furthermore, six rooftop PV systems with smaller capacities (around 9 to 12 MW) are implemented, which results in the total number of power converters considered in this scenario reaching 17. Similar to the previous scenario, a converter reliability with a large capacity can be derived from several converter reliability models where each has a small capacity.

B. Importance of Considering Converter Reliability

To highlight the importance of considering power converters when evaluating system reliability, traditional system indicators are calculated for all three scenarios, including EENS, and LOLE. Fig. 7 illustrates the accumulated EENS and LOLE for all three scenarios, respectively. The annual values of EENS
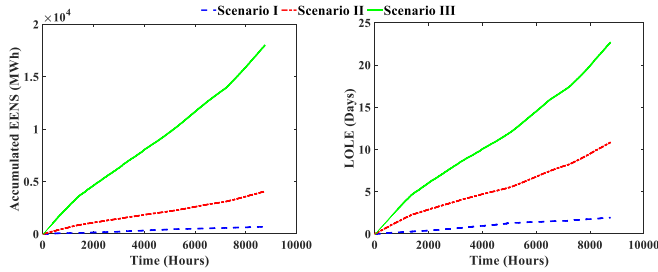
Fig. 7.   Accumulated EENS of all three scenarios.

TABLE I
RELIABILITY INDICATORS UNDER ALL SCENARIOS

Scenario	EENS (MWh/yr)	LOLE (days)	Number of Converters
I	695.74	1.94	\
II	4070.38	10.85	9
III	18025.91	22.68	17

TABLE II
TOTAL NUMBER OF DEVICES USED IN DIFFERENT CONVERTER TOPOLOGIES

Topology	IGBTs	Diodes	Capacitors
CHB	12	12	3
NPC	12	18	2
FCC	12	12	9

and LOLE are also summarized in Table I. In Fig. 7, the EENS and LOLE increase quickly in the last two scenarios while they are maintained at relatively low values in scenario I. This is because of the uncertainty of WT and PV systems, and the power converter failures being introduced in the last two scenarios. Additionally, the EENS in scenario I finally reaches 695.74 MWh/year and LOLE reaches 1.94 days, which are 17.1% and 17.9%, respectively, compared with scenario II, and 3.9% and 8.6% compared with scenario III. This shows that the power converter has a non-negligible effect on system reliability. As the number of power converters considered in the power system increases, both EENS and LOLE reach a relatively high value which indicates the system becoming unreliable.

C. The Reliability Effect of Converter Topologies

The converter topology not only determines how many power electronic devices are used but also reveals how they are connected with each other. Consequently, converter reliability performance can be greatly affected by the choice of converter topology. Thus, only scenario II and III are considered. Three typical converter topologies for high-power WTs and PVs are selected: a three-level cascaded H-bridge (CHB), a neutral point clamped (NPC), and a flying capacitor converter (FCC) [37], [38]. The total number of various devices used in these topologies are summarized in Table II.   NPC is also known as diode-clamped and more diodes are applied in this topology compared with in the other two topologies. The three-level FCC needs a minimum of four independent capacitors, i.e., a total of

TABLE III
ML REGRESSION RESULTS OF SVR AND RF

Model	Scenario	RMSE	R-squared
SVR	II	1.943	0.947
	III	2.719	0.892
RF	II	2.221	0.921
	III	2.895	0.883
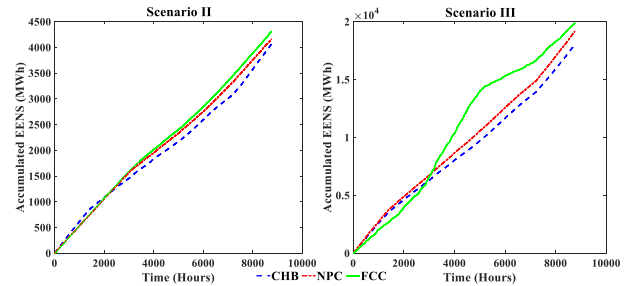
Fig. 8.   Scenario II EENS under three converter topologies.

two auxiliary capacitors per phase leg in addition to two main dc bus capacitors [37]. The detailed topology information of all three converter topologies can be reviewed in [38].

Fig. 8 illustrates the system EENS while three topologies are applied in scenario II and III, respectively, where the blue dotted line represents CHB, the red dash-dot line is NPC, and the green solid line depicts the FCC topology. The EENS value among all three topologies grow steadily and finally reaches 4070.38 MWh (CHB), 4164.07 MWh (NPC), and 4315.58 MWh (FCC) in Fig. 8, which indicates that the converter topologies do have an influence on system reliability, though, this influence is not very critical. Notably, in scenario III, the system EENS with FCC topology grows rapidly during 3000 to 5000 hours (summertime) and then slows down, which indicates an outage is more likely to happen during the summer and more maintenance may be required.

There are other power converter topologies that can be connected with RESs and implemented in a power system. It is to be noted, however, that the purpose of this case is not to find the optimal converter topology for power converters/system reliability performance, but to investigate system reliability when different converter topologies are applied.

D. The Regression Mapping Between Two Levels

To investigate the hidden relationship between device level and system level reliability, SVR and RF regression models are implemented. In general, 80% of the device/system reliability data is used for training as input variables to the model for intrinsic parameters selection. The remaining 20% is used for testing. The computational time of SVR and RF are 42.78 s and 45.64 s, respectively. Two statistical measurements: Root Mean Square Error (RMSE), and R-squared, are used to evaluate the effectiveness of the implemented regression methods.

In the numerical analysis, the RMSE values under scenario II are all lower than those values in scenario III. This is due to
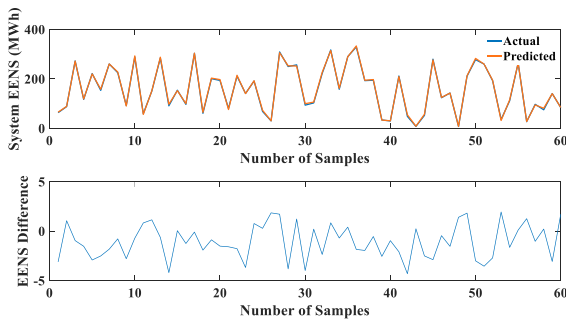
Fig. 9. Comparison of the predicted and the actual EENS.

the system complexity, i.e., fewer number of power converters is considered in scenario II. On the other hand, both R-squared values of SVR and RF methods reach above 0.9 in scenario II and 0.88 in scenario III, respectively. As shown in Fig. 9, 60 samples of testing data are collected to compare the predicted EENS and the corresponding actual value. The difference between the predicted and actual value is also shown in the same figure. In general, the predicted EENS follows the actual EENS pattern across all samples, and the maximum difference only reaches 4.31(absolute value). This indicates that it is possible to implement a reliability mapping between the power converter and system level through ML techniques.

VII. CONCLUSION

This paper proposes a two-level reliability framework to bridge the gap between power converters and power systems. The reliability performance of a power system is evaluated considering the impact of power converters' reliability. The reliability model of each converter is built from the device level, where critical semi-conductor devices are included. Each converter reliability is used as one of the input features and the system reliability indicators are defined to be the outputs. Furthermore, to investigate the relationship between converter and system reliability, ML regression techniques are used as it is a useful tool to determine nonlinear relationships. The numerical results show that the converter reliability has a non-negligible effect on the modern power system performance, and a nonlinear relationship between multiple power converters and overall system reliability can be built using regression techniques. Future works will focus on investigating the applications of parallel computing to speed up the proposed reliability analysis. The reliability impact of power converters' internal connections in a RES is also worth investigating. The influence on the power system network changes (i.e., different network topologies) will change the power flow and ultimately affect the system reliability performance. Once the real-world or synthetic transmission networks become available for reliability analysis, one will be able to investigate the scalability of the proposed reliability assessment framework. Moreover, since ML encapsulates the relationship and acts like a 'black box', the integration of ML interpreting methods will be investigated to improve the reliability explanation and provide useful information for system

operators. Appropriate reliability requirements on the converter level, and corresponding system maintenance strategies could be investigated.

REFERENCES

[1] G. Yingkui and L. Jing, "Multi-state system reliability: A new and systematic review," *Procedia Eng.*, vol. 29, pp. 531–536, 2012. [Online]. Available: https://core.ac.uk/download/pdf/82690643.pdf

[2] P. Zhou, R. Y. Jin, and L. W. Fan, "Reliability and economic evaluation of power system with renewables: A review," *Renewable Sustain. Energy Rev.*, vol. 58, pp. 537–547, 2016. [Online]. Available: https://ideas.repec.org/a/eee/rensus/v58y2016icp537-547.html

[3] J. Jaise, N. A. Kumar, N. S. Shanmugam, K. Sankaranarayanasamy, and T. Ramesh, "Power system: A reliability assessment using FTA," *Int. J. Syst. Assurance Eng. Manage.*, vol. 4, no. 1, pp. 78–85, 2013.

[4] J. Fang, C. Su, Z. Chen, H. Sun, and P. Lund, "Power system structural vulnerability assessment based on an improved maximum flow approach," *IEEE Trans. Smart Grid*, vol. 9, no. 2, pp. 777–785, Mar. 2018.

[5] A. Arabali, M. Ghofrani, M. Etezadi-Amoli, and M. S. Fadali, "Stochastic performance assessment and sizing for a hybrid power system of solar/wind/energy storage," *IEEE Trans. Sustain. Energy*, vol. 5, no. 2, pp. 363–371, Apr. 2014.

[6] F. A. O. Polo, J. F. Bermejo, J. F. G. Fernández, and A. C. Márquez, "Failure mode prediction and energy forecasting of PV plants to assist dynamic maintenance tasks by ANN based models," *Renewable Energy*, vol. 81, pp. 227–238, 2015.

[7] S. K. Awadallah, J. V. Milanović, and P. N. Jarman, "The influence of modeling transformer age related failures on system reliability," *IEEE Trans. Power Syst.*, vol. 30, no. 2, pp. 970–979, Mar. 2015.

[8] Y. Ding, C. Singh, L. Goel, J. Østergaard, and P. Wang, "Short-term and medium-term reliability evaluation for power systems with high penetration of wind power," *IEEE Trans. Sustain. Energy*, vol. 5, no. 3, pp. 896–906, Jul. 2014.

[9] A. Ahadi, N. Ghadimi, and D. Mirabbasi, "Reliability assessment for components of large scale photovoltaic systems," *J. Power Sour.*, vol. 264, pp. 211–219, 2014.

[10] B. Falahati, Y. Fu, and M. J. Mousavi, "Reliability modeling and evaluation of power systems with smart monitoring," *IEEE Trans. Smart Grid*, vol. 4, no. 2, pp. 1087–1095, Jun. 2013.

[11] S. Wang, Z. Li, L. Wu, M. Shahidehpour, and Z. Li, "New metrics for assessing the reliability and economics of microgrids in distribution system," *IEEE Trans. Power Syst.*, vol. 28, no. 3, pp. 2852–2861, Aug. 2013.

[12] B. Wang, J. Cai, X. Du, and L. Zhou, "Review of power semiconductor device reliability for power converters," *CPSS Trans. Power Electron. Appl.*, vol. 2, no. 2, pp. 101–117, 2017.

[13] D. Zhou, H. Wang, and F. Blaabjerg, "Mission profile based system-level reliability analysis of DC/DC converters for a backup power application," *IEEE Trans. Power Electron.*, vol. 33, no. 9, pp. 8030–8039, Sep. 2018.

[14] J. Sakly, A. B. B. Abdelghani, I. Slama–Belkhodja, and H. Sammoud, "Reconfigurable DC/DC converter for efficiency and reliability optimization," *IEEE J. Emerg. Sel. Topics Power Electron.*, vol. 5, no. 3, pp. 1216–1224, Sep. 2017.

[15] A. Sadeghfam, S. Tohidi, and M. Abapour, "Reliability comparison of different power electronic converters for grid-connected PMSG wind turbines," *Int. Trans. Elect. Energy Syst.*, vol. 27, no. 9, 2017, Paper 2359.

[16] E. Jamshidpour, P. Poure, and S. Saadate, "Photovoltaic systems reliability improvement by real-time FPGA-based switch failure diagnosis and fault-tolerant DC–DC converter," *IEEE Trans. Ind. Electron.*, vol. 62, no. 11, pp. 7247–7255, Nov. 2015.

[17] N. Gupta, R. Garg, and P. Kumar, "Sensitivity and reliability models of a PV system connected to grid," *Renewable Sustain. Energy Rev.*, vol. 69, pp. 188–196, 2017.

[18] K. Ni, Y. Hu, D. T. Lagos, G. Chen, Z. Wang, and X. Li, "Highly reliable back-to-back power converter without redundant bridge arm for doubly fed induction generator-based wind turbine," *IEEE Trans. Ind. Appl.*, vol. 55, no. 3, pp. 3024–3036, May-Jun. 2019.

[19] K. Fischer *et al.*, "Reliability of power converters in wind turbines: Exploratory analysis of failure and operating data from a worldwide turbine fleet," *IEEE Trans. Power Electron.*, vol. 34, no. 7, pp. 6332–6344, Jul. 2019.

[20] B. Mangu and B. G. Fernandes, "Multi-input transformer coupled DC-DC converter for PV-wind based stand-alone single-phase power generating system," in *Proc. IEEE Energy Convers. Congr. Expo.*, 2014, pp. 5288–5295.

[21] P. Tu, S. Yang, and P. Wang, "Reliability-and cost-based redundancy design for modular multilevel converter," *IEEE Trans. Ind. Electron.*, vol. 66, no. 3, pp. 2333–2342, Mar. 2019.

[22] S. E. De León-Aldaco, H. Calleja, and J. A. Alquicira, "Reliability and mission profiles of photovoltaic systems: A FIDES approach," *IEEE Trans. Power Electron.*, vol. 30, no. 5, pp. 2578–2586, May 2015.

[23] E. Ceperic, V. Ceperic, and A. Baric, "A strategy for short-term load forecasting by support vector regression machines," *IEEE Trans. Power Syst.*, vol. 28, no. 4, pp. 4356–4364, Nov. 2013.

[24] S. Peyghami, F. Blaabjerg, and P. Palensky, "Incorporating power electronic converters reliability into modern power system reliability analysis," *IEEE J. Emerg. Sel. Topics Power Electron.*, vol. 9, no. 2, pp. 1668–1681, Apr. 2021.

[25] N. Shahidirad, M. Niroomand, and R. A. Hooshmand, "Investigation of PV power plant structures based on Monte Carlo reliability and economic analysis," *IEEE J. Photovolt.*, vol. 8, no. 3, pp. 825–833, May 2018.

[26] N. Nguyen, S. Almasabi, J. Mitra, and B. B. Shenoy, "Correlation of wind speed and wind turbine reliability in system adequacy assessment," in *Proc. IEEE Int. Conf. Probabilistic Methods Appl. Power Syst.*, 2018, pp. 1–6.

[27] R. Billinton and G. Bai, "Generating capacity adequacy associated with wind energy," *IEEE Trans. Energy Conver.*, vol. 19, no. 3, pp. 641–646, Sep. 2004.

[28] H. Lei and C. Singh, "Non-sequential Monte Carlo simulation for cyber-induced dependent failures in composite power system reliability evaluation," *IEEE Trans. Power Syst.*, vol. 32, no. 2, pp. 1064–1072, Mar. 2017.

[29] D. Urgun and C. Singh, "A hybrid Monte Carlo simulation and multi label classification method for composite system reliability evaluation," *IEEE Trans. Power Syst.*, vol. 34, no. 2, pp. 908–917, Mar. 2019.

[30] L. Duchesne, E. Karangelos, and L. Wehenkel, "Machine learning of real-time power systems reliability management response," in *Proc. IEEE Manchester PowerTech*, 2017, pp. 1–6.

[31] T. Dragičević, P. Wheeler, and F. Blaabjerg, "Artificial intelligence aided automated design for reliability of power electronic systems," *IEEE Trans. Power Electron.*, vol. 34, no. 8, pp. 7161–7171, Aug. 2019.

[32] H. Liu *et al.*, "A nonlinear regression application via machine learning techniques for geomagnetic data reconstruction processing," *IEEE Trans. Geosci. Remote Sens.*, vol. 57, no. 1, pp. 128–140, Jan. 2019.

[33] H. Shaker, H. Zareipour, and M. Fotuhi-Firuzabad, "Reliability modeling of dynamic thermal rating," *IEEE Trans. Power Del.*, vol. 28, no. 3, pp. 1600–1609, Jul. 2013.

[34] N. Tomin, A. Zhukov, D. Sidorov, V. Kurbatsky, D. Panasetsky, and V. Spiryaev, "Random forest based model for preventing large-scale emergencies in power systems," *Int. J. Artifi. Intell.*, vol. 13, no. 1, pp. 211–228, 2015.

[35] L. Benali, G. Notton, A. Fouilloy, C. Voyant, and R. Dizene, "Solar radiation forecasting using artificial neural network and random forest methods: Application to normal beam, horizontal diffuse and global components," *Renew. Energy*, vol. 132, pp. 871–884, 2019.

[36] C. Grigg *et al.*, "The IEEE reliability test system-1996. A report prepared by the reliability test system task force of the application of probability methods subcommittee," *IEEE Trans. Power Syst.*, vol. 14, no. 3, pp. 1010–1020, Aug. 1999.

[37] M. Norambuena, S. Kouro, S. Dieckerhoff, and J. Rodriguez, "Reduced multilevel converter: A novel multilevel converter with a reduced number of active switches," *IEEE Trans. Ind. Electron.*, vol. 65, no. 5, pp. 3636–3645, May 2018.

[38] H. Watanabe, T. Sakuraba, K. Furukawa, K. Kusaka, and J. I. Itoh, "Development of DC to single-phase ac voltage source inverter with active power decoupling based on flying capacitor dc/dc converter," *IEEE Trans. Power Electron.*, vol. 33, no. 6, pp. 4992–5004, Jun. 2018.

Bowen Zhang (Student Member, IEEE) received the B.S. degree in electrical engineering from Southeast University, Nanjing, China, in 2015, and the M.S. degree in electrical engineering in 2017 from the University of Michigan-Dearborn, Dearborn, MI, USA, where he is currently working toward the Ph.D. degree in electrical engineering. His current research interests include power electronics, power system reliability, and machine learning.

Mengqi Wang (Senior Member, IEEE) received the B.S. degree in electrical engineering from Xi'an Jiaotong University, Xi'an, in 2009 and the Ph.D. degree in electrical engineering from North Carolina State University, Raleigh, NC, USA, in 2014. Since 2015, she has been an Assistant Professor with the Department of Electrical and Computer Engineering, University of Michigan-Dearborn, Dearborn, MI, USA, USA. Her research interests include dc–dc and dc–ac power conversions, high efficiency and high power-density power supplies, renewable energy systems, and wide-bandgap power device applications.

Wencong Su (Senior Member, IEEE) received the B.S. degree (with distinction) from Clarkson University, Potsdam, NY, USA, in 2008, the M.S. degree from Virginia Tech, Blacksburg, VA, USA, in 2009, and the Ph.D. degree from North Carolina State University, Raleigh, NC, USA, in 2013. He is currently an Associate Professor with the Department of Electrical and Computer Engineering, University of Michigan-Dearborn, Dearborn, MI, USA. He is a Fellow of IET. He is an Editor for the IEEE TRANSACTIONS ON SMART GRID, an Associate Editor for the IEEE ACCESS, and an Associate Editor of IEEE DataPort. He is a registered Professional Engineer (P.E.) in the State of Michigan, USA. His current research interests include power systems, electrified transportation systems, and cyber-physical systems. He was the recipient of the 2015 IEEE Power and Energy Society (PES) Technical Committee Prize Paper Award and the 2013 IEEE Industrial Electronics Society (IES) Student Best Paper Award.